Effect of regularization of Schmid law on self-consistent estimates for rate-independent plasticity of polycrystals

Kengo Yoshida, Renald Brenner, Brigitte Bacroix, Salima Bouvier

Accepted Manuscript

Title: Effect of regularization of Schmid law on self-consistent estimates for rate-independent plasticity of polycrystals

Authors: Kengo Yoshida, Renald Brenner, Brigitte Bacroix, Salima Bouvier

PII: S0997-7538(09)00061-8

DOI: 10.1016/j.euromechsol.2009.05.001

Reference: EJMSOL 2525

To appear in: *European Journal of Mechanics / A Solids*

Received Date: 30 January 2009

Revised Date: 28 April 2009

Accepted Date: 1 May 2009

Please cite this article as: Yoshida, K., Brenner, R., Bacroix, B., Bouvier, S. Effect of regularization of Schmid law on self-consistent estimates for rate-independent plasticity of polycrystals, European Journal of Mechanics / A Solids (2009), doi: 10.1016/j.euromechsol.2009.05.001

Effect of regularization of Schmid law on self-consistent estimates for rate-independent plasticity of polycrystals

Kengo Yoshida[a,b*], Renald Brenner[a], Brigitte Bacroix[a] and Salima Bouvier[a]

[a] LPMTM, CNRS, University Paris 13, 99 Avenue Jean-Baptiste Clement, 93430 Villetaneuse, France

[b] Forming Technologies R&D Center, Steel Research Laboratories, Nippon Steel Corporation, 20-1 Shintomi, Futtsu, Chiba 293-8511, Japan

*Corresponding author

Tel.: +33 1 49 40 34 67; Fax: +33 1 49 40 39 38.

E-mail address: yoshida.kengo1@nsc.co.jp (K. Yoshida).

Abstract

The mechanical response of an elastoplastic polycrystalline aggregate is estimated by means of Taylor and Hill's incremental self-consistent models in conjunction with two rate-independent crystal plasticity laws: standard and regularized Schmid laws. With the Taylor model, both constitutive laws lead to the same result whereas for the self-consistent model, the standard Schmid law predicts softer effective response than the regularized Schmid law and higher strain heterogeneity within the polycrystal. It is found that these features are related to the decrease of the shear tangent moduli during deformation when the standard Schmid law is considered. The presented results with the regularized Schmid law are in agreement with previous findings for power law viscoplastic polycrystals. It is demonstrated that the description of the crystal plasticity law significantly affects the estimate delivered by the Hill's incremental self-consistent model for elastoplastic polycrystals.

Keywords

Self-consistent model, rate-independent elastoplasticity, polycrystal, nonlinear homogenization

1. Introduction

Homogenization methods are efficient approaches to estimate the mechanical properties of heterogeneous materials. In the case of polycrystalline media, theoretical results have shown that the linear elastic self-consistent model (Hershey, 1954; Kröner, 1958) is well appropriated to describe their effective properties (Kröner, 1978). This has been assessed by comparing the effective behavior and the local fields with results delivered by full-field computations on various polycrystalline microstructures (see, for instance, Lebensohn et al., 2004; Castelnau et al., 2006; Brenner et al., submitted).

The extension of the self-consistent model to rate-independent elastoplastic behavior has first been proposed by Budiansky et al. (1960) and Kröner (1961) who investigated the early stage of plasticity by considering plastic grains interacting with an elastic matrix. To describe entirely the elastoplastic response of polycrystals, a seminal work was further introduced by Hill (1965) and Hutchinson (1970) who proposed an incremental approach based on the linear rate-form of local constitutive equations which rely on the Schmid law. More recently, an affine approach has been proposed by Masson et al. (2000) who showed, for a non-hardening f.c.c. polycrystal, that it leads to a lower steady-state effective yield stress than the incremental model.

In the related context of power-law viscoplastic f.c.c. polycrystals, various extensions of the self-consistent model, including the incremental (Hutchinson, 1976) and affine (Masson et al, 2000) approaches, have been compared to rigorous nonlinear bounds obtained with the variational procedure of Ponte Castañeda (1991). Nebozhyn et al. (2001) have shown that the incremental model violates the variational self-consistent estimate on the effective yield stress, which is an upper bound for all self-consistnet estimates, and tends to the Taylor bound in the rate-independent limit. By contrast, the affine model respects the available bounds, for this specific class of polycrystals. In view of these results, Hill's incremental model (1965) could be expected to present similar shortcomings in the context of rate-independent elastoplasticity. However, a few works (Hutchinson, 1970 and Takahashi, 1988) show that the incremental model estimates softer response than the Taylor bound for elastoplasticity, which contradicts

the above expectation. The link between the rate-independent limit of viscoplasticity and rate-independent elastoplasticity remains an open question.

In the present work, we analyze the influence of the local elastoplastic behavior on the incremental self-consistent estimate of the polycrystal response. For that goal, two rate-independent crystal plasticity models have been chosen. On one hand, use is made of the Standard Schmid Law (SSL) in which plastic slip is considered to occur on a slip system when the resolved shear stress reaches a critical value. This constitutive law leads multi-yield functions and the determination of the slip rates is an inverse problem of the constraint conditions. The constraints can be linearly dependent and result in the non-uniqueness of the set of active slip systems when the hardening matrix is not positive definite (Hill, 1966). This has led to various proposals for the hardening description (see, for instance, Franciosi and Zaoui, 1991; Bassani, 1994) and for the technique to identify the set of slip systems (Anand and Kothari, 1996; Miehe and Schröder, 2001; Busso and Cailletaud, 2005). A simple and often used method to circumvent this difficulty is to forsake the rate-independent formulation and adopt a power-law type rate-dependent viscoplastic formulation (see, for instance, Asaro and Needleman, 1985). On the other hand, Regularized Schmid Law (RSL) has been proposed to overcome this problem within the framework of the rate-independent plasticity (see, Gambin, 1992; Darrieulat and Piot, 1996; Franz et al. 2009). The advantage of the regularization is that it does not involve the problem of linear dependence. It has been used in the homogenization context with the Taylor model (Darrieulat and Piot, 1996, Kowalczyk and Gambin, 2004), the Transformation Field Analysis (Franciosi and Berbenni, 2007) and, recently, the self-consistent model (Franz et al. 2009). In section 2, two crystal-plasticity models (SSL and RSL) are presented and the corresponding tangent moduli in the rate-form constitutive relations are compared for single and double slip cases in the single crystal context. These crystal plasticity laws are then introduced in the Taylor and incremental self-consistent models and the mechanical responses of two different non-hardening f.c.c. polycrystals are estimated (Sections 3 and 4). The significance of the description of constitutive law, especially the instantaneous tangent moduli, on the self-consistent estimates is discussed in details in section 5.

2. Rate-independent crystal plasticity models

2.1. Framework of crystal plasticity model

In this study, we confine attention to small strain conditions. The strain rate is given by the symmetry part of $\partial \mathbf{v}/\partial \mathbf{x}$, where $\mathbf{v}$ and $\mathbf{x}$ are velocity and position, respectively. We consider additive decomposition of strain rate into elastic and plastic parts.

$$\dot{\boldsymbol{\varepsilon}} = \dot{\boldsymbol{\varepsilon}}^{\mathrm{e}} + \dot{\boldsymbol{\varepsilon}}^{\mathrm{p}}. \tag{1}$$

Elastic relation is given by Hooke's law.

$$\dot{\boldsymbol{\sigma}} = \mathbf{C}^{\mathrm{e}} : \dot{\boldsymbol{\varepsilon}}^{\mathrm{e}} = \mathbf{C}^{\mathrm{e}} : (\dot{\boldsymbol{\varepsilon}} - \dot{\boldsymbol{\varepsilon}}^{\mathrm{p}}), \tag{2}$$

where $\mathbf{C}^{\mathrm{e}}$ is the forth-order elastic moduli tensor.

Crystallographic slips are considered to be the source for the plastic deformation, and the plastic strain rate takes the form

$$\dot{\boldsymbol{\varepsilon}}^{\mathrm{p}} = \sum_{\alpha} \dot{\gamma}^{(\alpha)} \mathbf{p}^{(\alpha)}, \tag{3}$$

$$\mathbf{p}^{(\alpha)} := \frac{1}{2}(\mathbf{s}^{(\alpha)} \otimes \mathbf{m}^{(\alpha)} + \mathbf{m}^{(\alpha)} \otimes \mathbf{s}^{(\alpha)}), \tag{4}$$

where $\dot{\gamma}^{(\alpha)}$, $\mathbf{s}^{(\alpha)}$ and $\mathbf{m}^{(\alpha)}$ are the slip rate, the slip direction and the slip plane normal for the α th slip system, respectively. The resolved shear stress for the α th slip system, $\tau^{(\alpha)}$, is written as

$$\tau^{(\alpha)} = \mathbf{s}^{(\alpha)} \cdot \boldsymbol{\sigma} \cdot \mathbf{m}^{(\alpha)} = \boldsymbol{\sigma} : \mathbf{p}^{(\alpha)}, \tag{5}$$

where $\boldsymbol{\sigma}$ is true stress. From Equations (3) and (5), a resolved shear stress rate is given as

$$\dot{\tau}^{(\alpha)} = \mathbf{p}^{(\alpha)} : \mathbf{C}^{\mathrm{e}} : \dot{\boldsymbol{\varepsilon}} - \sum_{\beta} \dot{\gamma}^{(\beta)} \mathbf{p}^{(\alpha)} : \mathbf{C}^{\mathrm{e}} : \mathbf{p}^{(\beta)}, \tag{6}$$

where $\mathbf{s}^{(\alpha)}$ and $\mathbf{m}^{(\alpha)}$ are assumed to be constant. Slip resistance for the α th slip system is denoted by $g^{(\alpha)}$, and its evolution is governed by

$$\dot{g}^{(\alpha)} = \sum_{\beta} h^{\alpha\beta} |\dot{\gamma}^{(\beta)}|, \tag{7}$$

where $h^{\alpha\beta}$ denotes hardening moduli.

2.2. Standard Schmid law

For a crystal plasticity model based on the standard Schmid law, the local yield function, f, is written as

$$f = \sup_{\alpha=1,\cdots,N^{s}} f^{(\alpha)} = 0, \tag{8}$$

with

$$f^{(\alpha)} = |\tau^{(\alpha)}| - g^{(\alpha)} = 0, \tag{9}$$

where N^{s} is the number of slip systems and $f^{(\alpha)}$ is a yield function for each slip system. The plastic strain rate is given by

$$\dot{\boldsymbol{\varepsilon}}^{p} = \sum_{\alpha} \mathrm{sgn}(\tau^{(\alpha)}) \dot{\gamma}^{(\alpha)} \mathbf{p}^{(\alpha)}, \tag{10}$$

where slip rates, $\dot{\gamma}^{(\alpha)}$, are assumed to be positive. It is worth noting that the above equation can be derived from the normality rule if the yield function for each slip system is considered as a potential: $\dot{\boldsymbol{\varepsilon}}^{p} = \sum_{\alpha} \dot{\gamma}^{(\alpha)} (\partial f^{(\alpha)} / \partial \boldsymbol{\sigma})$.

Based on N^{s} independent yield functions (Equation (9)) potentially active and inactive slip systems are classified as

$$\dot{\gamma}^{(\alpha)} \geq 0, \quad \text{for } f^{(\alpha)} = 0 \text{ and } \dot{f}^{(\alpha)} = 0, \tag{11a}$$

$$\dot{\gamma}^{(\alpha)} = 0, \quad \text{for } f^{(\alpha)} < 0, \text{ or } f^{(\alpha)} = 0 \text{ and } \dot{f}^{(\alpha)} < 0. \tag{11b}$$

From the consistency condition of the yield functions, the slip rates, $\dot{\gamma}^{(\alpha)}$, on the active slip systems are determined as

$$\dot{f}^{(\alpha)} = R^{\alpha} - \sum_{\beta} X^{\alpha\beta} \dot{\gamma}^{(\beta)} = 0, \tag{12}$$

$$\dot{\gamma}^{(\alpha)} = \sum_{\beta} Y^{\alpha\beta} R^{(\beta)} , \tag{13}$$

where

$$R^{(\alpha)} := \mathrm{sgn}(\tau^{(\alpha)}) \mathbf{p}^{(\alpha)} : \mathbf{C}^{\mathrm{e}} : \dot{\boldsymbol{\varepsilon}} , \tag{14a}$$

$$X^{\alpha\beta} := h^{\alpha\beta} + \mathrm{sgn}(\tau^{(\alpha)}) \mathrm{sgn}(\tau^{(\beta)}) \mathbf{p}^{(\alpha)} : \mathbf{C}^{\mathrm{e}} : \mathbf{p}^{(\beta)} , \tag{14b}$$

$$[Y^{\alpha\beta}] := [X^{\alpha\beta}]^{-1} , \tag{14c}$$

where $(\bullet)^{-1}$ denotes the inverse. Under a particular hardening rule, $h^{\alpha\beta}$, $X^{\alpha\beta}$ may become singular, and this results in a possible non-uniquess of the set of the active slip systems for a given deformation mode. But for perfect plasticity, $h^{\alpha\beta} = 0$, it is always possible to choose at least one set of linearly independent slip systems from the potentially active slip systems such that $X^{\alpha\beta}$ is non-singular and Equations (11) are satisfied (Hutchinson, 1970). If there are greater than five linearly independent systems, five slip systems are selected in the computations[1].

Using equations (2), (10) and (13), we finally obtain the rate-form of the constitutive equation, $\dot{\boldsymbol{\sigma}} = \mathbf{L} : \dot{\boldsymbol{\varepsilon}}$, in term of the elastoplastic tangent moduli,

$$\mathbf{L} := \mathbf{C}^{\mathrm{e}} - \sum_{\alpha} \left\{ \left(\mathrm{sgn}(\tau^{(\alpha)}) \mathbf{C}^{\mathrm{e}} : \mathbf{p}^{(\alpha)} \right) \otimes \sum_{\beta} \left(\mathrm{sgn}(\tau^{(\beta)}) Y^{\alpha\beta} \mathbf{p}^{(\beta)} : \mathbf{C}^{\mathrm{e}} \right) \right\} . \tag{15}$$

2.3. Regularized Schmid law

In order to avoid the possible singularity of $X^{\alpha\beta}$ in the Schmid law, a regularized Schmid law for rate-independent crystal plasticity was proposed (Gambin, 1992). The following

[1] For comparison purpose we use the same approach as Hutchinson's (1970). In a preliminary study, different criteria have been used for the selection of the five active slip systems, and it has been confirmed that the choice of the criterion does not have any influence on the estimation.

157 regularized yield function is introduced.

158 $$f = \left\{ \sum_{\alpha} \left(\frac{\tau^{(\alpha)}}{g^{(\alpha)}} \right)^{2N} \right\}^{\frac{1}{2N}} - 1 = 0 , \tag{16}$$

159 where N is an integer parameter so that the exponent always becomes an even number. The
160 plastic strain rate is assumed to be given by

161 $$\dot{\boldsymbol{\varepsilon}}^{\mathrm{p}} = \sum_{\alpha} \dot{\gamma}^{(\alpha)} \mathbf{p}^{(\alpha)} , \tag{17}$$

162 and follows, on the other hand, from the normality rule associated with the yield function
163 (16),

164 $$\dot{\boldsymbol{\varepsilon}}^{\mathrm{p}} = \dot{\Lambda} \frac{\partial f}{\partial \boldsymbol{\sigma}} . \tag{18}$$

165 From these two expressions of the plastic strain rate, the slip rate on a given slip system reads

166 $$\dot{\gamma}^{(\alpha)} = \frac{\dot{\lambda}}{g^{(\alpha)}} \left(\frac{\tau^{(\alpha)}}{g^{(\alpha)}} \right)^{2N-1} \quad \text{with} \quad \dot{\lambda} = \dot{\Lambda} \left\{ \sum_{\alpha} \left(\frac{\tau^{(\alpha)}}{g^{(\alpha)}} \right)^{2N} \right\}^{\frac{1}{2N}-1} , \tag{19}$$

167 where $\dot{\lambda}$ is a positive plastic multiplier. By contrast to the SSL, slip rates for all the slip
168 systems derived from a unique plastic multiplier. Therefore, there is no need to classify active
169 and inactive slip systems among the set of slip systems. Equation (19) is similar to the one
170 describing vicsoplastic crystal (e.g. Asaro and Needleman, 1985) in which a reference slip
171 rate is introduced instead of a plastic multiplier.
172
173 Loading-unloading conditions are written as

174 $$\dot{\lambda} \geq 0 , \quad \text{for} \quad f = 0 \quad \text{and} \quad \dot{f} = 0 , \tag{20a}$$

175 $$\dot{\lambda} = 0 , \quad \text{for} \quad f < 0 , \text{or} \quad f = 0 \quad \text{and} \quad \dot{f} < 0 . \tag{20b}$$

176 From the consistency condition of the yield function, the plastic multiplier, $\dot{\lambda}$, is determined.

177 $$\dot{f} = \mathbf{G} : \mathbf{C}^{\mathrm{e}} : \dot{\boldsymbol{\varepsilon}} - \dot{\lambda} (\mathbf{G} : \mathbf{C}^{\mathrm{e}} : \mathbf{G} + H) = 0 , \tag{21}$$

$$\dot{\lambda} = \frac{\mathbf{G} : \mathbf{C}^{\mathrm{e}} : \dot{\boldsymbol{\varepsilon}}}{\mathbf{G} : \mathbf{C}^{\mathrm{e}} : \mathbf{G} + H}, \tag{22}$$

where

$$\mathbf{G} := \sum_{\alpha} \left\{ \left(\frac{\tau^{(\alpha)}}{g^{(\alpha)}} \right)^{2N-1} \frac{\mathbf{p}^{(\alpha)}}{g^{(\alpha)}} \right\}, \tag{23a}$$

$$H := \sum_{\alpha} \left[\left(\frac{\tau^{(\alpha)}}{g^{(\alpha)}} \right)^{2N} \frac{1}{g^{(\alpha)}} \sum_{\beta} \left\{ \frac{h_{\alpha\beta}}{g^{(\beta)}} \left(\frac{|\tau^{(\beta)}|}{g^{(\beta)}} \right)^{2N-1} \right\} \right]. \tag{23b}$$

In the derivation of $\dot{\lambda}$, any inverse of a matrix is not required. Namely, the difficulty related to the linearly dependence in the Schmid law is avoided.

We finally obtain the rate-form constitutive equation for a single crystal, $\dot{\boldsymbol{\sigma}} = \mathbf{L} : \dot{\boldsymbol{\varepsilon}}$, in terms of the elastoplastic tangent moduli,

$$\mathbf{L} := \mathbf{C}^{\mathrm{e}} - \frac{(\mathbf{C}^{\mathrm{e}} : \mathbf{G}) \otimes (\mathbf{G} : \mathbf{C}^{\mathrm{e}})}{\mathbf{G} : \mathbf{C}^{\mathrm{e}} : \mathbf{G} + H}. \tag{24}$$

2.3. Comparison of Schmid and regularized Schmid laws

In this subsection, the standard Schmid and regularized Schmid laws are compared in terms of yield locus, active slip systems and tangent moduli. The SSL gives multi-plane yield locus which possesses corners, while the RSL gives a smooth yield locus with rounded corners. The curvature of the rounded corner for the RSL increases with the exponent N, and when N is large enough, the smooth yield locus is in good agreement with the multi-plane SSL's one (Darrieulat and Piot, 1996; Gambin and Barlat, 1997). Besides, although all the slip systems are active if the yield condition is satisfied, finite slips take place only on the slip systems where $\tau^{(\alpha)} \approx g^{(\alpha)}$ when the exponent N is large, while slip rates for the other slip systems, where $\tau^{(\alpha)} < g^{(\alpha)}$, are close to zero (Equation (19)). This is similar to the Schmid law, for which slip system activates when $\tau^{(\alpha)} = g^{(\alpha)}$. Therefore, the yield locus and active slip systems corresponding to the Schmid law are correctly described by the regularized Schmid law when $N \to +\infty$. On the contrary, the tangent moduli given in Equation (15) and (24) are not identical a priori. To be more specific, the tangent moduli given by the two laws are compared for some special cases.

(i) Single slip case

Let us consider a crystal that possesses a single slip system. The exponent in the regularized Schmid law is taken to $N = +\infty$. In this case, the yield function (16) reduces to Equation (9). It is assumed that $\tau^{(1)} = g^{(1)}$ and $\dot{\tau}^{(1)} = \dot{g}^{(1)}$ for the slip system. This situation results in the activation of the slip system for both SSL and RSL. Then the tangent moduli is written as

$$\mathbf{L} = \mathbf{C}^{\mathrm{e}} - \frac{(\mathbf{C}^{\mathrm{e}} : \mathbf{p}^{(1)}) \otimes (\mathbf{p}^{(1)} : \mathbf{C}^{\mathrm{e}})}{\mathbf{p}^{(1)} : \mathbf{C}^{\mathrm{e}} : \mathbf{p}^{(1)} + h^{11}}. \tag{25}$$

The tangent moduli (15) and (24) are reduced to the same equation.

(ii) Double slip case

Next, let us consider a crystal that possesses two slip systems. It is assumed that $\tau^{(1)} = g^{(1)}$, $\tau^{(2)} = g^{(2)}$ and $\dot{\tau}^{(1)} = \dot{g}^{(1)}$, $\dot{\tau}^{(2)} = \dot{g}^{(2)}$. For both the Schmid and regularized Schmid laws, the yield criteria are satisfied and slips occur for both the first and second slip systems. These situations are similar to that for the single slip case. In this case, the tangent moduli obtained with the Schmid law (Equation(15)) reduces to

$$\mathbf{L} = \mathbf{C}^{\mathrm{e}} - \mathbf{C}^{\mathrm{e}} : \{\mathbf{p}^{(1)} \otimes (Y^{11}\mathbf{p}^{(1)} + Y^{12}\mathbf{p}^{(2)}) + \mathbf{p}^{(2)} \otimes (Y^{21}\mathbf{p}^{(1)} + Y^{22}\mathbf{p}^{(2)})\} : \mathbf{C}^{\mathrm{e}}, \tag{26}$$

where

$$\begin{bmatrix} Y^{11} & Y^{12} \\ Y^{21} & Y^{22} \end{bmatrix} = \begin{bmatrix} h^{11} + \mathbf{p}^{(1)} : \mathbf{C}^{\mathrm{e}} : \mathbf{p}^{(1)} & h^{12} + \mathbf{p}^{(1)} : \mathbf{C}^{\mathrm{e}} : \mathbf{p}^{(2)} \\ h^{21} + \mathbf{p}^{(2)} : \mathbf{C}^{\mathrm{e}} : \mathbf{p}^{(1)} & h^{22} + \mathbf{p}^{(2)} : \mathbf{C}^{\mathrm{e}} : \mathbf{p}^{(2)} \end{bmatrix}^{-1}, \tag{27}$$

and $g^{(1)} = g^{(2)}$ is assumed for simplicity.

With the regularized Schmid law, the tangent moduli (Equation(24)) gives

$$\mathbf{L} = \mathbf{C}^{\mathrm{e}} - \frac{\mathbf{C}^{\mathrm{e}} : (\mathbf{p}^{(1)} + \mathbf{p}^{(2)}) \otimes (\mathbf{p}^{(1)} + \mathbf{p}^{(2)}) : \mathbf{C}^{\mathrm{e}}}{(\mathbf{p}^{(1)} + \mathbf{p}^{(2)}) : \mathbf{C}^{\mathrm{e}} : (\mathbf{p}^{(1)} + \mathbf{p}^{(2)}) + h_{11} + h_{12} + h_{21} + h_{22}}. \tag{28}$$

For the double slip case, the two crystal plasticity laws do not give the identical expression of tangent moduli. For the Schmid law, interaction of $\mathbf{p}^{(\alpha)}$ for each slip system appears with different coefficient, $Y^{\alpha\beta}$, while interaction of the summation of $\mathbf{p}^{(\alpha)}$ emerges for the regularized Schmid law.

The tangent moduli given by the two laws are calculated for a special case shown in Figure 1 (a). Two slip systems are arranged symmetrically about the x_1 axis and slip directions and slip plane normals are in the $x_1 - x_2$ plane, that is, $\mathbf{s}^{(1)} = (\cos\phi, \sin\phi, 0)$ $\mathbf{m}^{(1)} = (\sin\phi, -\cos\phi, 0)$, $\mathbf{s}^{(2)} = (\cos\phi, -\sin\phi, 0)$ and $\mathbf{m}^{(2)} = (\sin\phi, \cos\phi, 0)$. For simplicity, isotropic elasticity and non-hardening is assumed. Then, analytical expression of tangent moduli are written as

$$L_{1111} = L_{2222} = L_{1122} = \lambda + \mu, \tag{29a}$$

$$L_{1212} = \begin{cases} C^{\mathrm{e}}_{1212} - \mu = 0 & \text{for the Schmid law} \\ C^{\mathrm{e}}_{1212} = \mu & \text{for the regularized Schmid law} \end{cases} \tag{29b}$$

$$L_{ijkl} = C^{\mathrm{e}}_{ijkl} \quad \text{for others components} \tag{29c}$$

where λ and μ are Lamé constants. The difference of tangent modulus is appeared for L_{1212} component.

In the derivation of the analytical expression of the tangent moduli $N = +\infty$ is assumed, however, a finite value of N is required in actual computation. In order to check the sensitivity of N, the same problem is solved numerically with $N = 500$. Parameters are set to $\phi = 15°$, $E/\tau_0 = 1000$, $\nu = 1/3$ and $h^{\alpha\beta} = 0$, where E, ν and τ_0 are the Young's modulus, Poisson's ratio and critical resolved shear stress, respectively. Uniaxial tension in the x_1 direction is applied. Figure 1(b) shows the tangent moduli normalized by E as a function of the tensile strain. Tangent moduli given by the two crystal plasticity laws coincide except for the L_{1212} component, and L_{1212} for the Schmid law decrease to zero when the yield condition is satisfied, whereas that for the regularized Schmid law remains constant. The tangent moduli computed with $N = 500$ coincide with those obtained analytically with $N = +\infty$. Figure 1(c) shows the good agreement between SSL and RSL tensile flow stresses. Thus, the yield stress and active slip systems are the same for both crystal plasticity laws whereas the shear tangent moduli are different.

Following these comparisons at the single crystal level, the question which arises is the

influence, if any, of the different instantaneous local tangent moduli on the polycrystal response. To tackle this problem, use will be made of the Taylor and self-consistent models which are briefly described in the next section.

3. Homogenization estimates

3.1. Self-consistent model

In this study, we mainly focus on the role of the crystal plasticity law on the local and effective response for the elastoplastic polycrystalline aggregate. Consequently, the Hill's (1965) incremental self-consistent model, which is up to now the most widely used model for elastoplastic polycrystal, is adopted. Polycrystal is considered to consist of ellipsoidal phases which compose grains orientating at the same direction. In the self-consistent model, an ellipsoidal phase is assumed to be embedded in an infinite linear comparison homogenous medium which has a unique tangent moduli corresponding to the effective tangent ones. The phase average stress and strain rates can be related to the macroscopic ones through the localization tensors, $\mathbf{A}^r$ and $\mathbf{B}^r$,

$$<\dot{\boldsymbol{\varepsilon}}>^r = \mathbf{A}^r : \dot{\bar{\boldsymbol{\varepsilon}}}, \quad <\dot{\boldsymbol{\sigma}}>^r = \mathbf{B}^r : \dot{\bar{\boldsymbol{\sigma}}}, \tag{30}$$

where the superscript r refers to the quantity for the r th phase, a bar indicates a macroscopic value and $<\bullet>$ stands for a volume average. The rate-form constitutive equation is used to represent linear relationship between the stress and strain rates. The constitutive equations of a phase and effective medium are respectively denoted as

$$<\dot{\boldsymbol{\sigma}}>^r = \mathbf{L}^r :< \dot{\boldsymbol{\varepsilon}}>^r, \tag{31}$$

$$\dot{\bar{\boldsymbol{\sigma}}} = \tilde{\mathbf{L}} : \dot{\bar{\boldsymbol{\varepsilon}}}, \tag{32}$$

with

$$\tilde{\mathbf{L}} :=< \mathbf{L}^r : \mathbf{A}^r >. \tag{33}$$

where $\mathbf{L}^r$ and $\tilde{\mathbf{L}}$ are the tangent moduli of a phase and effective medium, respectively. $\mathbf{L}^r$ is assumed to be homogeneous within a phase and can be calculated by Equation (15) or (24) replacing the local quantities with the phase average ones, for instance, a resolved shear stress $<\tau^{(\alpha)}>^r = \mathbf{p}^{(\alpha)} :< \boldsymbol{\sigma} >^r$ is used instead of $\tau^{(\alpha)} = \mathbf{p}^{(\alpha)} : \boldsymbol{\sigma}$. The strain localization tensor is given

by

$$\mathbf{A}^r = \{\mathbf{I} + \mathbf{P} : (\mathbf{L}^r - \tilde{\mathbf{L}})\}^{-1}. \tag{34}$$

where $\mathbf{I}$ is fourth-order identity tensor and $\mathbf{P}$ is so called Hill's tensor described as

$$\mathbf{P} = \int_\Omega \mathbf{\Gamma}\, \mathrm{d}V, \tag{35}$$

where

$$\Gamma_{ijkl} \coloneqq \frac{1}{4}(K_{ik}^{-1}\xi_j\xi_l + K_{jk}^{-1}\xi_i\xi_l + K_{il}^{-1}\xi_j\xi_k + K_{jl}^{-1}\xi_i\xi_k), \tag{36a}$$

$$\mathbf{K} \coloneqq \boldsymbol{\xi}\cdot\tilde{\mathbf{L}}\cdot\boldsymbol{\xi}, \tag{36b}$$

where Ω is the domain within a phase and $\boldsymbol{\xi}$ is a position vector on the surface of inclusion (see, for instance, Mura, 1982). This set of relations defines a nonlinear systems for the average strain rates per phase, $<\dot{\boldsymbol{\varepsilon}}>^r$, which can be solved using a fixed-point iterative algorithm.

3.2. Taylor model

In the Taylor model, $\mathbf{A}^r = \mathbf{I}$ is assumed, that is, the local strain field is taken to be identical to the macroscopic one,

$$\dot{\boldsymbol{\varepsilon}} = <\dot{\boldsymbol{\varepsilon}}>^r = \dot{\bar{\boldsymbol{\varepsilon}}}. \tag{37}$$

Then, the effective tangent moduli in the rate-form of constitutive equation, $\dot{\bar{\boldsymbol{\sigma}}} = \tilde{\mathbf{L}} : \dot{\bar{\boldsymbol{\varepsilon}}}$, are given by

$$\tilde{\mathbf{L}} = <\mathbf{L}>. \tag{38}$$

Since the local strain field is known a priori, iterative computation is not needed for the Taylor model.

In the next section, the Taylor and incremental self-consistent models described above are used in conjunction with SSL and RSL for estimating the mechanical behavior of f.c.c. polycrystals at both local and overall scales.

4. Results

4.1. Uniaxial tension for non-hardening f.c.c. polycrystalline aggregate

Macroscopically isotropic polycrystal is considered. Its microstructure is represented by 216 crystalline phases with same volume fractions. Besides, a spherical shape is assumed for the each phase. A non-hardening ($h^{\alpha\beta}=0$) f.c.c. crystal with 12 slip systems, $\{111\}<110>$, is assumed for each phase, and slip resistances are set as $g^{(\alpha)}=\tau_0$, where τ_0 is a critical resolved shear stress. For simplicity isotropic elasticity with $E/\tau_0=1000$ and $\nu=1/3$ is considered. The exponent in the regularized Schmid laws is $N=500$. (The effect of the exponent, N, on homogenization estimates is discussed in Appendix.) Mechanical response of the polycrystal subjected to the uniaxial tension in the x_1 direction is simulated with the Taylor and self-consistent models in conjunction with the Schmid and regularized Schmid laws.

Figure 2 shows the macroscopic uniaxial stress-strain curve, where the flow stress is normalized by critical resolved shear stress, τ_0. For the Taylor model, the flow stresses predicted by both the Schmid and regularized Schmid laws are in good agreement. Since $N=500$ is large enough, the regularized Schmid law approaches Schmid one as is mentioned in section 2. The flow stresses, eventually, saturate to the value of 3.06, which is the same as the well-known Taylor factor for rigid-plastic f.c.c. polycryatal.

For the self-consistent model, plastic yielding occur earlier than for the Taylor model and the estimation of flow stress significantly depend on the crystal plasticity laws used in the analysis. When the Schmid law is used, softer response is obtained. Indeed, the normalized flow stress saturate to the value of 2.82. On the contrary, when the regularized Schmid law is used, stiffer response is predicted and the stress state asymptotically approaches the one predicted by the Taylor model. When the regularized Schmid law is used, the Taylor and self-consistent models estimate almost the same behavior for the large strain range.

By definition, local strain states are the same as macroscopic one for the Taylor model and vary for the self-consistent model. Figure 3 shows the evolution of local strain component

normalized by the macroscopic tensile strain for the self-consistent model. The normalized strain components for 216 phases are depicted. During the whole tensile straining process, the Schmid law based self-consistent model predicts about $\pm 15\%$ of constant variation of local strain field. On the other hand, for the regularized Schmid law, similar variation is predicted just after plastic yielding, but then the variation shrinks. At $\bar{\varepsilon}_{11} = 0.05$, the variation is less than $\pm 2\%$. Thus, the self-consistent model with the regularized Schmid law is closer to the Taylor model in terms of local field fluctuation. This small strain heterogeneity is consistent with the macroscopic stress-strain curve that approaches the one of the Taylor model.

The local strain rate is specified by localization tensor in Equation (34), which includes the local and effective tangent moduli and Hill's $\mathbf{P}$ tensor. The $\mathbf{P}$ tensor reflects the difference of the local and effective tangent moduli to the localization tensor. The higher the components of $\mathbf{P}$ are, the more enhanced the strain heterogeneity is. Components of $\mathbf{P}$ are shown in Figure 4. For the Schmid model, the absolute value of the $\mathbf{P}$ components increase with tensile straining. On the other hand, for the RSL, the $\mathbf{P}$ components are almost constant and small. Therefore, the localization tensor is close to unit tensor and the fluctuation of local strain field is small. The evolution of $\mathbf{P}$ tensor is in agreement with the local strain variation in Figure 3.

As is shown in the equations (35) and (36), the $\mathbf{P}$ tensor depends on the effective tangent moduli. Figure 5 shows the estimated effective tangent moduli in the rate-form of the constitutive equations. The tangent moduli, $\tilde{L}_{ijkl}$, are normalized by the elastic moduli, C^{e}_{ijkl}. For the uniaxial tensile loading, the macroscopic tangent moduli display transverse isotropy with respect to the x_1 direction, that is, $\tilde{L}_{2222} = \tilde{L}_{3333}$, $\tilde{L}_{1122} = \tilde{L}_{1133}$ and $\tilde{L}_{1212} = \tilde{L}_{1313}$. The tangent moduli predicted by the two crystal plasticity laws do not agree except for 1111 and 1122 components. Both tangent moduli depicted in Figure 5 correspond to uniaxial tension state although they are not identical. The most significant difference is the shear tangent moduli: those obtained with the Schmid law rapidly decrease after plastic yielding and eventually reach to zero, whereas those for the regularized Schmid law are almost constant during deformation. This trend is the same as that for the simple double slip case depicted in

Figure 1(b). General relationships between $\mathbf{P}$ and $\tilde{\mathbf{L}}$ are given in Equations (35) and (36) and analytical expressions can be found by Hutchinson (1970) for transverse isotropic symmetry. $\mathbf{P}$ tensor increases when $\tilde{\mathbf{L}}$ decreases, thus the lower $\tilde{\mathbf{L}}$ components pronounce a deviation of the localization tensor from the identity tensor.

For the Taylor model, SSL and RSL give the identical behavior so long as the exponent is high enough. However, for the self-consistent model, the description of the tangent moduli affects the local strain heterogeneity as well as effective response.

4.2. Polycrystalline aggregate with an elastic phase

In this subsection, the polycrystal aggregate is assumed to consist of 216 elastoplastic phases and an elastic phase. The elastic phase is considered in order to increase the contrast of the mechanical properties among phases. The volume fraction of the elastic phase is 0.3 and that of the other 216 phases are 0.00324. The material properties of the 216 elastoplastic phases are the same as ones in 4.1, and the same elastic properties are assigned to an elastic phase. All phases have spherical shape. Uniaxial tension in the x_1-direction is analyzed by means of the self-consistent model. Taylor model is not used here because the uniform strain field assumption is far from the reality for this problem.

Figure 6 shows the normalized flow stress as a function of the macroscopic tensile strain. The Schmid law based model predicts softer response than that for the regularized Schmid law. The qualitative tendency is the same as in Figure 2, and the existence of an elastic phase enhances the difference of effective response. Figure 7 shows the local strain distribution of the 216 elastoplastic and the elastic phases. The strain variation among the elastoplastic phases is larger for the Schmid law than the regularized Schmid law. For the Schmid law, the strain evolution in an elastic phase decreases with tensile strain, and the strain is much smaller than that for the elastoplastic phases. On the other hand, for the regularized Schmid law the strain develops linearly and its amount is about half of the elastoplastic phases. The Schmid law allows lager strain heterogeneity among elastoplastic phases as well as between elastoplastic and elastic phases. Figure 8 shows the effective shear tangent moduli normalized

by the same way as in 4.1. Again, the shear moduli decrease rapidly after yielding for the Schmid law, whereas those for the regularized Schmid law are almost constant. The influence of the tangent moduli emerges again for this problem and the strong contrast of the phases enhances this effect on the local and effective response.

5. Discussion

The description of standard Schmid law and regularized Schmid law has been examined for a uniaxial tensile loading (Section 2). It has become clear that both laws predict the same mechanical behavior of single grain under given boundary conditions, provided that the exponent in the regularized Schmid law is high enough. But, it has to be recalled that the tangent moduli given by the two laws are different, although the same response is predicted. For the non-hardening polycrystalline aggregate, the two laws with the Taylor model lead to the same mechanical response under uniaxial tension. This can be explained by the fact that, by definition, each phase undergoes the same strain field with the Taylor assumption. Since the SSL and RSL predict the same response for a phase under the same boundary conditions, the same mechanical response is predicted for each phase and consequently, the same local and effective responses are obtained for the polycrystal.[2] On the other hand, the two crystal plasticity laws lead to different estimates with the incremental self-consistent model. The shear tangent moduli for the SSL are lower than those for the RSL and are used to obtain strain localization tensors which specify the average strain field within a phase. Therefore, with the self-consistent model, the average strain field of a given phase varies between the SSL and RSL. Furthermore, the lower the tangent moduli are, the more the strain heterogeneity is enhanced. As a consequence, the self-consistent model with the SSL leads to the larger strain heterogeneity and softer overall response. On the other hand, the self-consistent model with the RSL predicts a smaller strain heterogeneity and a flow stress approaching to the upper bound. From this point of view, it can be concluded that the self-consistent model based on the SSL gives a better estimation.

[2] Uniaxial tensile behavior is also computed for the static model, which assumes a uniform stress field within the polycrystal. SSL and RSL with $N = 500$ estimate the same behavior and the macroscopic stress is stationary at $\bar{\sigma}_{11} / \tau_0 = 2$.

There are some similarities in the constitutive equations for the RSL and a power law viscoplasticity model: (i) the slip law in equation (19) and the one for viscoplascity both obey a power law, (ii) the regularized Schmid law possesses a smooth yield locus and the viscoplastic model presents a smooth equal potential locus in stress space. The power law viscoplastic model can thus also be considered as a regularization of the Schmid law. Numerous investigations have been performed on the self-consistent model in the viscoplastic context (see, among others, Hutchinson, 1976; Masson et al., 2000; Nebozhyn et al., 2001) and it has been shown that the effective yield stress predicted by the Hill's incremental model in the rate-independent limit is very close to the Taylor bound. By noting that this effective yield stress corresponds to the saturated flow stress of a non-hardening elastoplastic polycrystal, it is pointed out that our self-consistent estimates with a RSL are fully consistent with the results obtained in the viscoplastic context. Following these remarks, it is likely that any regularization (i.e. single yield function with associated flow rule) would lead to incremental self-consistent estimates with the same shortcomings than the one reported in the present study.

The physical interpretation of the reduced shear tangent moduli is considered here. First, a situation is assumed such that the double slip single grain shown in Figure 1(a) is continuously subjected to the uniaxial tension, and instantly shear strain rate, $\dot{\varepsilon}_{12}$, is applied additionally. Schematic illustration of yield surfaces for the RSL and SSL in $\sigma_{11}-\sigma_{12}$ space are shown in Figure 9. In these circumstances, the stress state is uniaxial tension, i.e. $\sigma_{ij}=0$ except for σ_{11}, and non-zero strain rate components are $\dot{\varepsilon}_{11}$, $\dot{\varepsilon}_{22}$ and $\dot{\varepsilon}_{12}$. For the RSL, the direction of the plastic strain rate is normal to the yield surface at the current stress state and $\dot{\varepsilon}_{12}^{\mathrm{p}}$ is not produced, hence $\dot{\varepsilon}_{12}$ is accomplished by elastic strain rate, $\dot{\varepsilon}_{12}^{\mathrm{e}}$. Thus, the tangent modulus of L_{1212} is identical to the elastic shear modulus. On the other hand, for the RSL, the direction of plastic strain rate lies between the normal directions of the facets. Therefore, when $\dot{\varepsilon}_{12}$ is applied, $\dot{\varepsilon}_{12}^{\mathrm{p}}$ is produced and the tangent modulus is consequently reduced. The introduction of the regularization, which avoids the difficulty of the selection of active slip systems, loses the vertex effect on the tangent moduli.

459

460 It is interesting to note an analogy between the standard and regularized Schmid laws and the
461 phenomenological J_2 flow and J_2 deformation theories. Reduced tangent moduli were
462 observed by Hutchinson (1970) who compared tangent moduli for the J_2 flow and
463 deformation theories. The flow theory assumes a smooth yield locus and associated flow rule
464 and the deformation theory reflects the point vertex effect on the yield surface. The flow and
465 deformation theories predict respectively constant and decreasing shear tangent moduli during
466 plastic deformation. The flow and deformation theories are similar to the RSL and SSL,
467 respectively. In fact, there is a vertex on the yield locus for the SSL and a single smooth yield
468 locus and associated flow rule are assumed in the RSL (Equations (16) and (18)).

469

470 In the crystalline context, our results highlight the fact that the flow stress estimate obtained
471 with a regularized crystal plasticity law can be different from the one that is obtained with the
472 non-smooth multi-criteria yield function corresponding to the SSL. In particular, the
473 incremental self-consistent model is significantly affected by the mathematical description of
474 the constitutive model and does not always lead to a stiff overall response with respect to the
475 Taylor model. Indeed, with the incremental self-consistent model, the Schmid law gives a
476 saturated flow stress of 2.82, which is lower than the estimation derived from the viscoplastic
477 power law in the rate-independent limit (≈ 3.06). Interestingly, it is noted that the saturated
478 flow stress obtained with the SSL does not violate the variational self-consistent estimate of
479 Ponte Castañeda for viscoplastic behavior which is equal to 2.948 in the rate-independent
480 limit (Nebozhyn et al. 2001). To give an insight on the pertinence of Hill's incremental model
481 in the framework of the standard Schmid law, it would be necessary to compare the
482 self-consistent estimate of the saturated flow stress with more rigorous bounds: the one
483 derived for polycrystalline materials exhibiting a rigid-plastic behavior with a multi-criteria
484 local yield function (see, for instance, Nesi et al., 2000) or the recent improvement of the
485 variational approach of Ponte Castañeda (Idiart and Ponte Castañeda 2007a,b) which was
486 shown to improve on earlier bounds in the case of a two-phase porous crystalline material.

487

488 Concerning the RSL, it is interesting to note that different studies on particulate composites

(matrix-inclusion microstructure) (Gonzales and LLorca, 2000; Doghri and Ouaar, 2003; Chaboche et al., 2005) with an elastoplastic matrix obeying the J_2 flow theory have shown that the incremental model deliver a too stiff overall stress-strain response by comparison with finite element computations. This is qualitatively in agreement with our results obtained by RSL for non-hardening polycrystal with an elastic phase. To obtain better self-consistent estimates, it would be necessary to incorporate the field heterogeneity in the nonlinear homogenization procedure for elastoplasticity.

6. Concluding remarks

The mechanical response of polycrystals has been investigated using the Hill's incremental self-consistent model in conjunction with different rate-independent crystal plasticity laws. The investigation of standard and regularized Schmid laws has revealed that they deliver the same plastic deformation behavior but different tangent moduli. The use of these two constitutive laws to describe the elastoplastic behavior of a non-hardening f.c.c. polycrystal has shown that the standard Schmid law predicts a wider heterogeneity of the local strain field and a softer overall response. We found that the reduced shear tangent moduli are responsible for this behavior. The incorporation of an elastic phase in the elastoplastic polycrystal allowed us to point out that an increase of the mechanical contrast implies a more pronounced influence of the tangent moduli on the self-consistent description. The shear tangent moduli decrease with the deformation for the SSL and remain constant for the RSL. With the incremental self-consistent model, the Schmid law gives a saturated flow stress which is lower than the estimation derived from the viscoplastic power law in the rate-independent limit. The saturated flow stress obtained with the SSL (Hutchinson, 1970) does not violate the variational self-consistent estimate of Ponte Castañeda for viscoplastic behavior in the rate-independent limit. Comparisons with more restrictive bounds are thus required.

7. Acknowledgements

The authors acknowledge Nippon Steel Corporation for a financial support to this study.

8. References

Anand, L., and Kothari, M., 1996. A computational procedure for rate-independent crystal plasticity. Journal of the Mechanics and Physics of Solids, 44(4), 525-558.

Asaro, R., and Needleman, A., 1985, Texture development and strain hardening in rate dependent polycrystals. Acta Metallurgica 33(6), 923-953.

Bassani, J.L., 1994. Plastic flow of crystals. In: Advances in Applied Mechanics, Volume 30. Academic Press, London, pp. 191-258.

Brenner, R., Lebensohn, R. A., Castelnau O., Elastic anisotropy and yield surface estimates of polycrystals, submitted.

Budiansky, B., Hashin, Z. and Sanders, J. L., 1960. The stress field of a slipped crystal and the early plastic behavior of polycrystalline materials Plasticity. In: Proceedings of the 2nd Symp Naval Struct Mech., Pergamon, Oxford, 1960, 239.

Busso, E. P. and Cailletaud, G., 2005. On the selection of active slip systems in crystal plasticity. Internatinal Journal of Plasticity 21(11), 2212-2231.

Castelnau, O., Brenner, R. and Lebensohn, R.A., 2006. The effect of strain heterogeneity on the work hardening of polycrystals predicted by mean-field approaches. Acta Materialia, 54(10) 2745-2756.

Chaboche, J.L., Kanoute, P., Roos A., 2005. On the capabilities of mean-field approaches for the description of plasticity in metal matrix composites. International Journal of Plasticity 21 (7) 1409-1434.

Darrieulat, M., Piot, D., 1996. A method of generating analytical yield surfaces of crystalline materials. International Journal of Plasticity 12(5) 575-610.

Doghri, I., Ouaar, A., 2003. Homogenization of two-phase elasto-plastic composite materials and structures, Study of tangent operators, cyclic plasticity and numerical algorithms. International Journal of Solids and Structures 40 (7) 1681-1712.

Franciosi, P. and Berbenni, S., 2007. Heterogeneous crystal and poly-crystal plasticity modeling from a transformation field analysis within a regularized Schmid law. Journal of the Mechanics and Physics of Solids, 55(11) 2265-2299.

Franciosi, P. and Zaoui A., 1991. Crystal hardening and the issue of uniqueness. International Journal of Plasticity, 7(4) 295-311.

548 Franz, G., Abed-Meraim, F., Lorrain, J.-P., Ben Zineb T., Lemoine, X. and Berveiller, M.,
549 2009. Ellipticity loss analysis for tangent moduli deduced from a large strain
550 elastic–plastic self-consistent model, International Journal of Plasticity, 25(2) 205-238.
551 Gambin, W., 1992. Refined analysis of elastic-plastic crystals, International Journal of Solids
552 and Structures 29 (16) 2013-2021.
553 Gambin, W., Barlat, F., 1997. Modeling of deformation texture development based on rate
554 independent crystal plasticity. International Journal of Plasticity 13(1-2) 75-85.
555 Gonzalez, C., LLorca, J., 2000. A self-consistent approach to the elasto-plastic behaviour of
556 two-phase materials including damage. Journal of the Mechanics and Physics of Solids
557 48 (4) 675-692.
558 Hershey, A.V., 1954. The elasticity of an isotropic aggregate of anisotropic cubic crystals,
559 Journal of Applied Mechanics, 21(9) 236-240
560 Hill, R., 1965. Continuum micro-mechanics of elastoplastic polycrystals. Journal of the
561 Mechanics and Physics of Solids, 13(2) 89-101.
562 Hill, R. 1966. Generalized constitutive relations for incremental deformation of metal crystals
563 by multislip. Journal of the Mechanics and Physics of Solids, 14(2), 95-102.
564 Hutchinson, J.W., 1970. Elastic-plastic behaviour of polycrystalline metals and composites.
565 Proceedings of the Royal Society of London A 319(1537) 247-272.
566 Hutchinson, J.W., 1976. Bounds and self-consistent estimates for creep of polycrystalline
567 materials. Proceedings of the Royal Society of London A 348(1652) 101-127.
568 Idiart, M.I. and Ponte Castañeda, P., 2007. Variational linear comparison bounds for nonlinear
569 composites with anisotropic phases. I. General results. Proceedings of the Royal Society
570 A, 463(2080), 907-924.
571 Idiart, M.I. and Ponte Castañeda, P., 2007. Variational linear comparison bounds for nonlinear
572 composites with anisotropic phases. II. Crystalline materials. Proceedings of the Royal
573 Society A, 463(2080), 925-943.
574 Kowalczyk, K. and Gambin, W., 2004. Model of plastic anisotropy evolution with
575 texture-dependent yield surface Int. J. Plasticity, 20(1), 19-54.
576 Kröner, E., 1958, Berechnung der elastischen Konstanten des Vielkristalls aus den Konstanten
577 des Einkristalls Z. Physik, 151, 504-518.

Kröner, E., 1961. Zur plastischen Verformung des Vielkristalls. Acta Metallurgica, 9(2) 155-191.

Kröner, E., 1978. Self-consistent scheme and graded disorder in polycrystal elasticity. Journal of Physics F: Metal Physics, 8(11), 2261-2267.

Lebensohn, R.A., Liu, Y. and Ponte Castañeda, P., 2004. On the accuracy of the self-consistent approximation for polycrystals: comparison with full-field numerical simulations, Acta Materialia, 52(18) 5347-5361.

Masson, R., Bornert, M., Suquet, P. and Zaoui, A., 2000. An affine formulation for the prediction of the effective properties of nonlinear composites and polycrystals. Journal of the Mechanics and Physics of Solids 48(6-7), 1203-1227.

Miehe, C. and Schröder, J., 2001. A comparative study of stress update algorithms for rate-independent and rate-dependent crystal plasticity. International Journal for Numerical Methods in Engineering 50(2)273-298.

Mura, T, 1982, Micromechanics of defects in solids. Martinus Nijhoff Publishers, The Hague.

Nebozhyn, M. V., Gilormini, P. and Ponte Castañeda, P., 2001. Variational self-consistent estimates for cubic viscoplastic polycrystals : the effects of grain anisotropy and shape. Journal of the Mechanics and Physics of Solids, 49(2), 313-340.

Nesi, V., Smyshlyaev, V.P. and Willis J.R., 2000. Improved bounds for the yield stress of a model polycrystalline material. ournal of the Mechanics and Physics of Solids 48(9), 1799-1825.

Ponte Castañeda, P., 1991. The effective mechanical properties of nonlinear isotropic composite. Journal of the Mechanics and Physics of Solids, 39(1), 45-71.

Takahashi, H., 1988. Predictions of plastic stress-strain relations of polycrystals based on the Lin model. International Journal of Plasticity, 4(3), 231-250.

Appendix

A1. Influence of exponent, N, in regularized Schmid law

The exponent, N, in the regularized Schmid law has been taken to 500 for the all computations in Section 4. In this section, N is taken to 5 and 50 in order to examine its influence on the microscopic and macroscopic mechanical responses, and the problems in

Section 4.1 and 4.2 are simulated. Figure A1(a) shows the macroscopic uniaxial stress-strain curve for the isotropic non-hardening crystalline aggregate. The saturated flow stresses predicted with the Taylor and self-consistent models coincide with each other for the same N and decrease with N. When $N = 5$, the flow stresses predicted by the Taylor and self-consistent models are softer than the one predicted by the self-consistent model with the Schmid law (Figure 2), since the yield stress of a single crystal becomes lower with decreasing the exponent. Thus, this prediction does not imply that the regularized Schmid law with $N = 5$ is capable of predicting the softer effective response with large strain heterogeneity. The development of the phase average strain for $N = 5$ is shown in Figure A1(b). The phase average strains once have a variation in the range of -20% to +10% just after the plastic yielding and then, the variation shrinks. The amount of strain heterogeneity is the same magnitude as the one for $N = 500$ in Figure 3(b). The strain heterogeneity for $N = 50$, which is not shown in the present paper, is almost the same as that for $N = 500$. Therefore, it is concluded that the exponent, N, has little influence on the estimation of mechanical response.

The microscopic and macroscopic deformation of polycrystals reinforced by an elastic inclusion, which is the problem in Section 4.2, is also simulated for $N = 5$ and 50, and the results are shown in Figure A2. Softer behavior is predicted for the case of $N = 5$, since lower exponent gives softer flow stress for a single crystal. Figure A2(b) shows the strain distribution in the polycrystalline and elastic phases. The predicted strain heterogeneity is almost the same as the one for $N = 500$ shown in Figure 7(b). We again conclude that the exponent, N, in the regularized Schmid law has almost no influence on the estimation of the mechanical behavior.

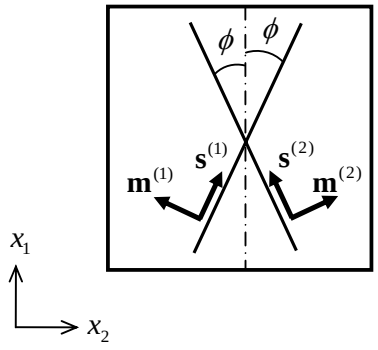

(a)

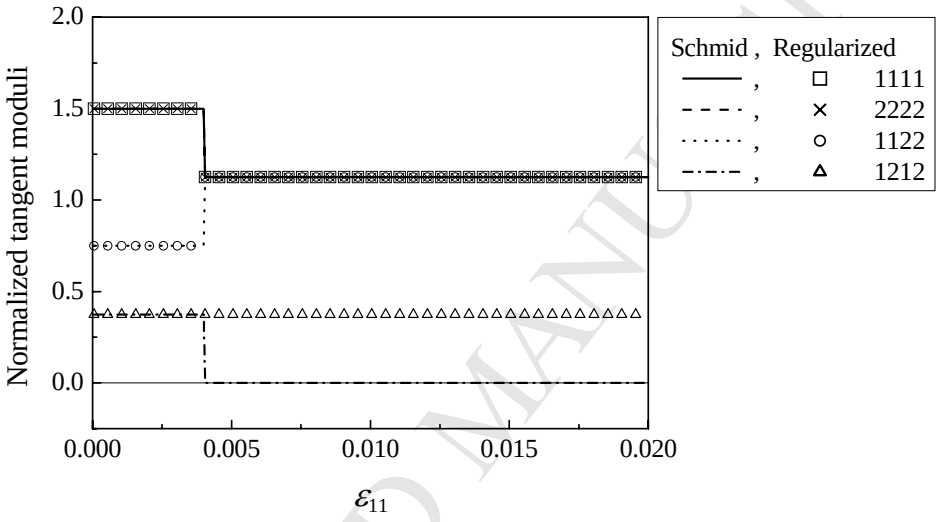

(b)

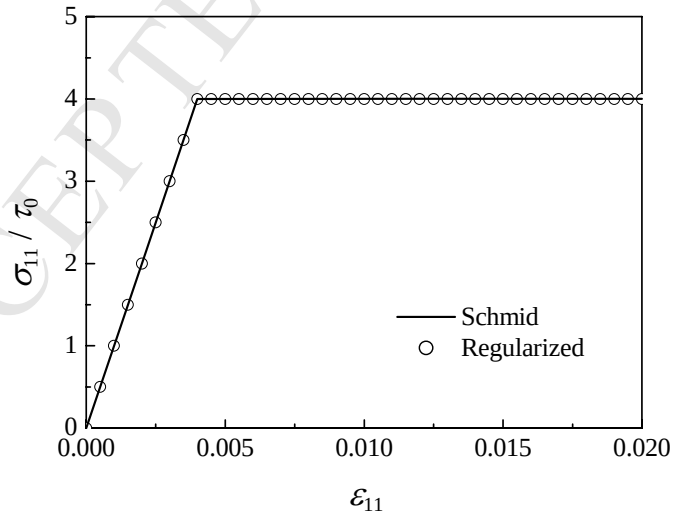

(c)

Figure 1. Tangent moduli for a double slip crystal under uniaxial tension. (a) Geometry of slip systems, (b) tangent moduli normalized by the Young's modulus and (c) tensile stress normalized by a critical resolved shear stress as a function of tensile strain.

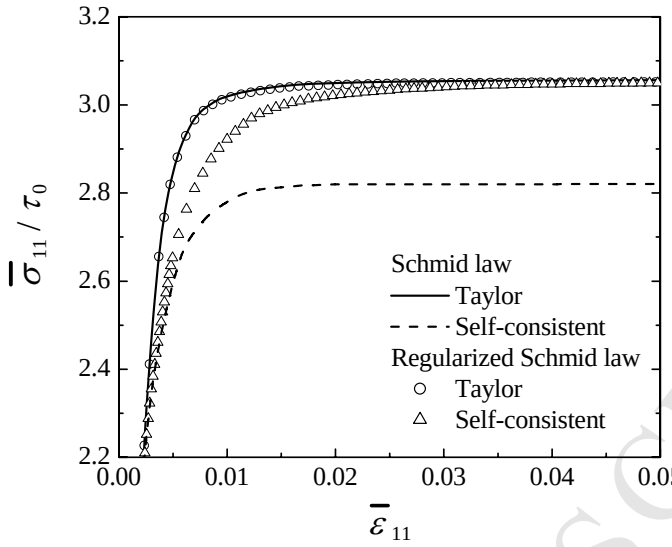

Figure 2. Macroscopic uniaxial stress-strain curve for isotropic non-hardening f.c.c. crystalline aggregate. Taylor and incremental self-consistent models are used in conjunction with Schmid and regularized Schmid laws.

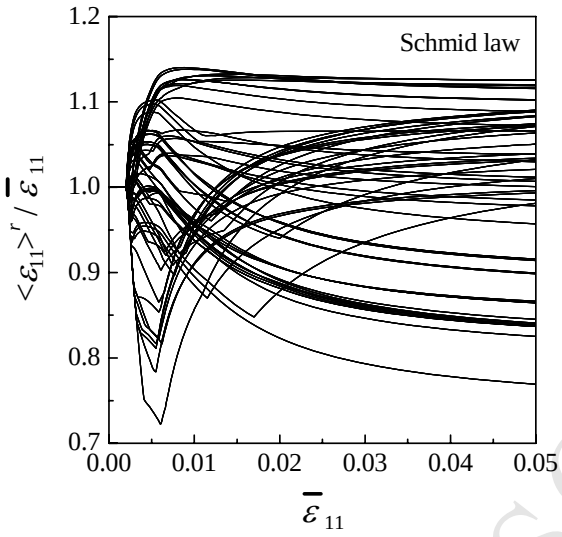

(a)

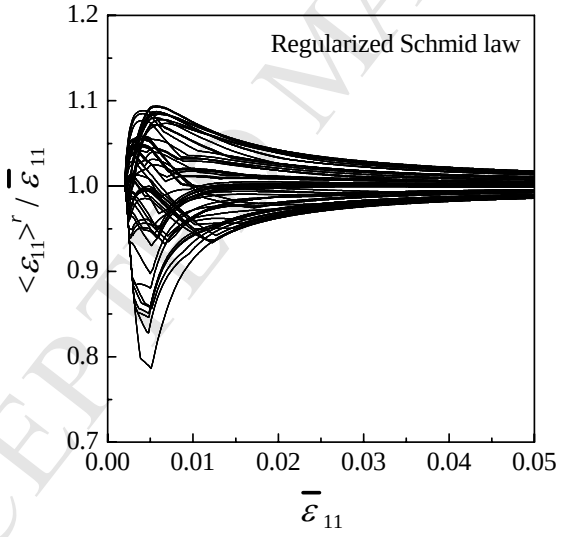

(b)

Figure 3. Evolution of local strain component, $<\varepsilon_{11}>^r$, in 216 phases under uniaxial tension. Incremental self-consistent model is used in conjunction with (a) Schmid law and (b) regularized Schmid law.

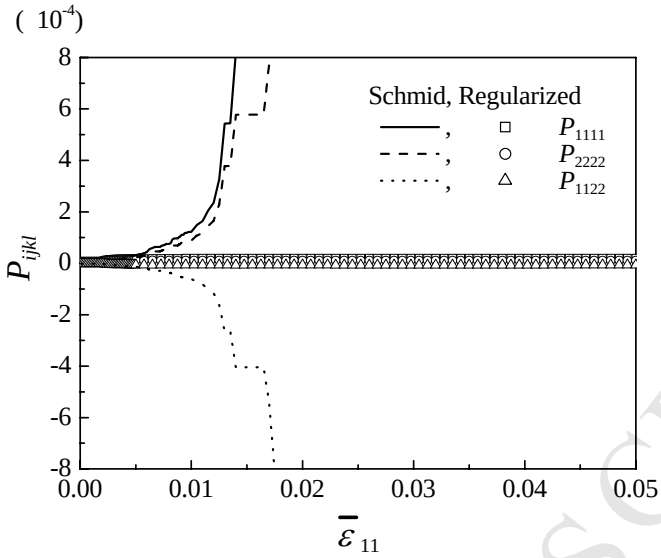

(a)

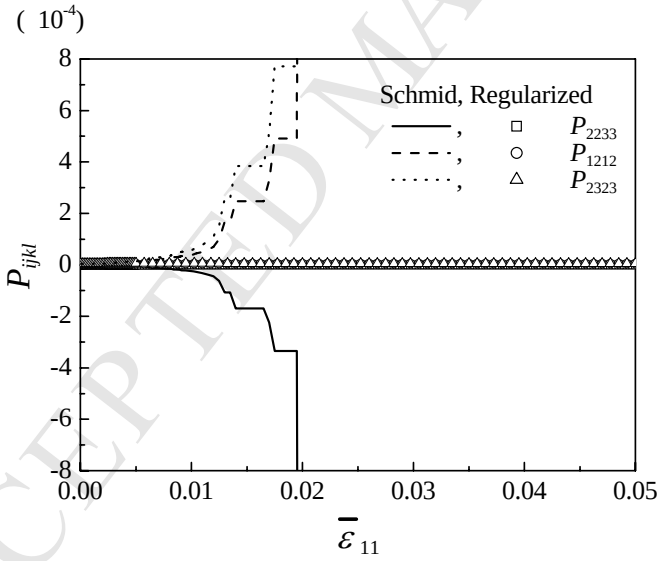

(b)

Figure 4. Evolution of **P** tensor for uniaxial tension as a function of macroscopic tensile strain.

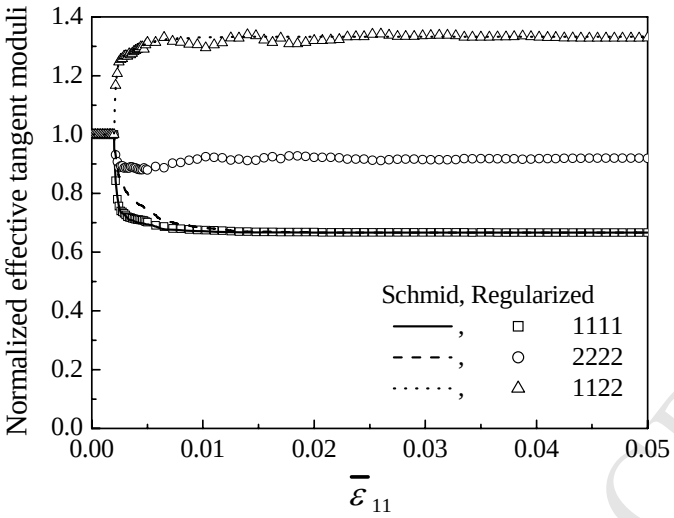

(a)

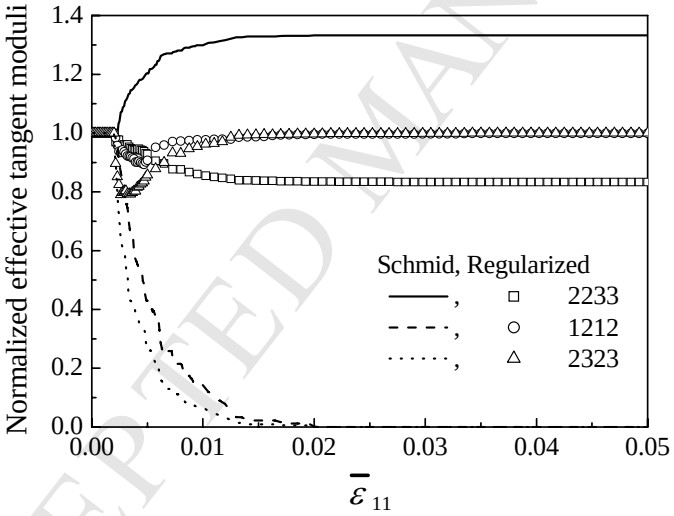

(b)

Figure 5. Evolution of tangent moduli under uniaxial tension. Effective tangent moduli, $\tilde{L}_{ijkl}$, are normalized by corresponding elastic moduli, C^{e}_{ijkl}.

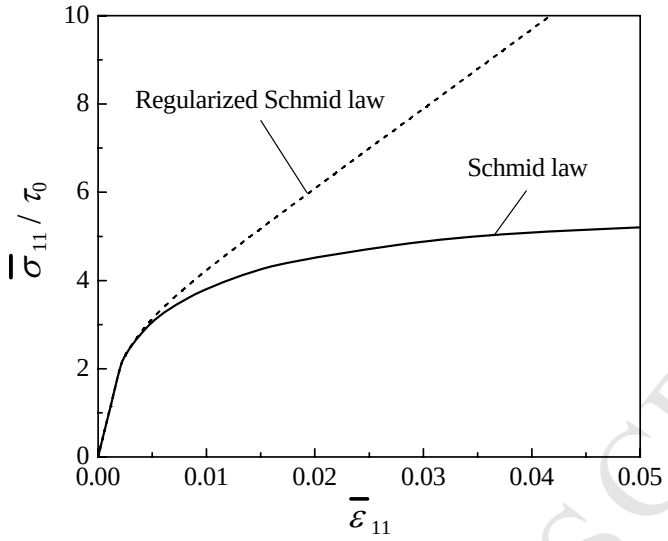

Figure 6. Stress-strain curve for aggregate consisting of elastoplastic phases and an elastic phase. Incremental self-consistent model is used in conjunction with Schmid and regularized Schmid laws.

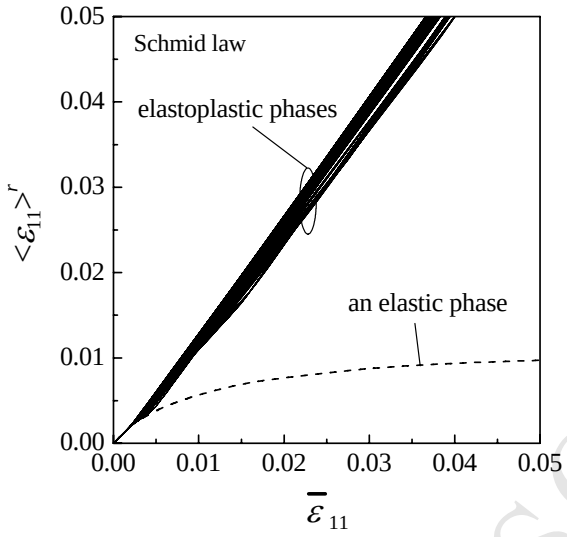

(a)

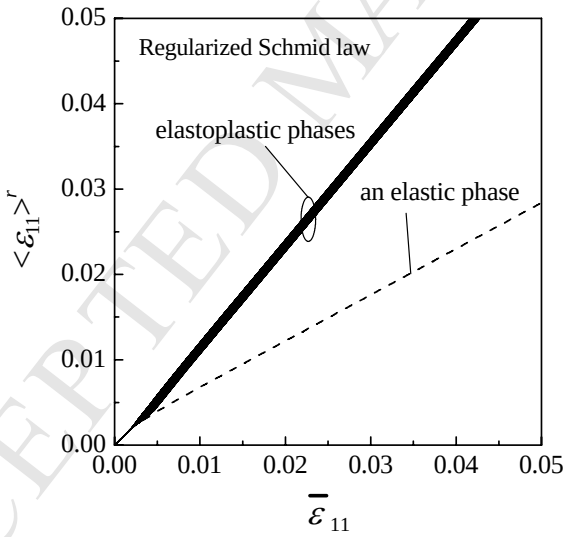

(b)

Figure 7. Evolution of local strain component, $<\varepsilon_{11}>^r$, in 216 elastoplastic phases and an elastic phase under uniaxial tension. Incremental self-consistent model is used in conjunction with (a) Schmid law and (b) Regularized Schmid law.

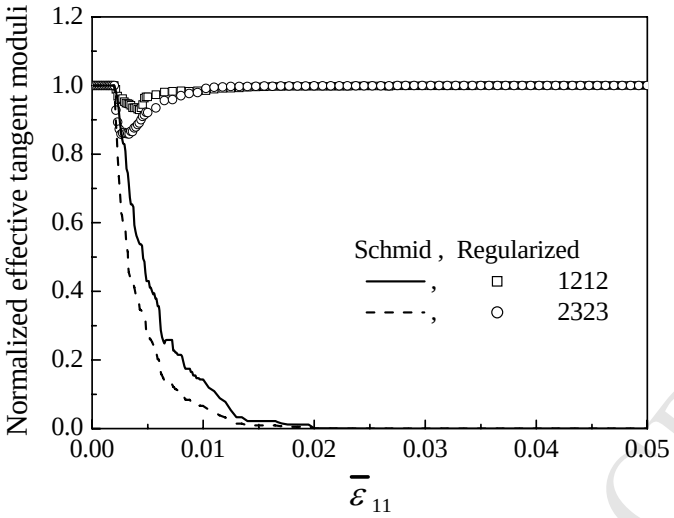

Figure 8. Evolution of tangent moduli for aggregate consisting of 216 elastoplastic phases and an elastic phase under uniaxial tension. Effective tangent moduli, $\tilde{L}_{ijkl}$, are normalized by elastic moduli, C^{e}_{ijkl}, for each component.

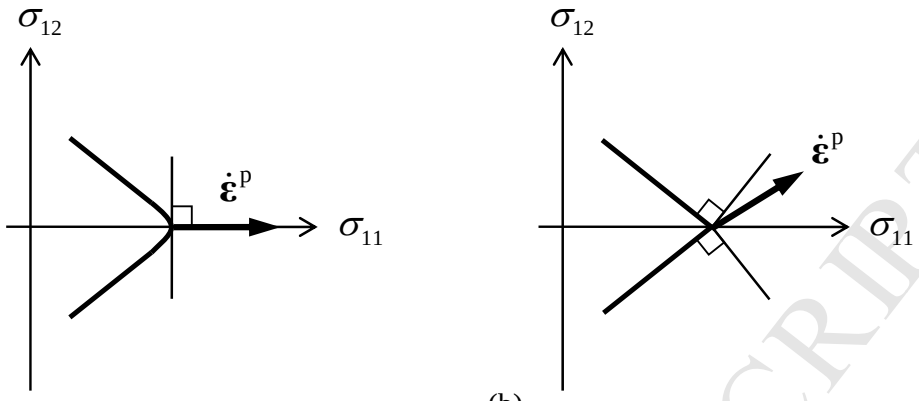

Figure 9. Schematic illustration of yield surface in $\sigma_{11}-\sigma_{12}$ space based on (a) regularized and (b) standard Schmid laws for a double slip crystal shown in Figure 1.

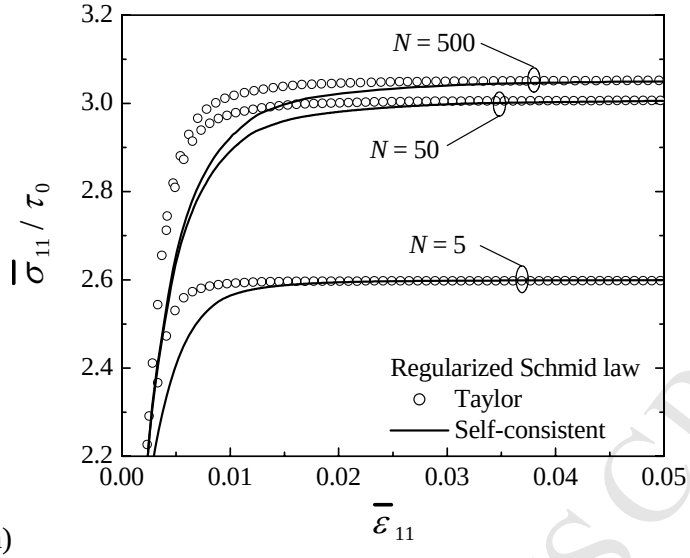

(a)

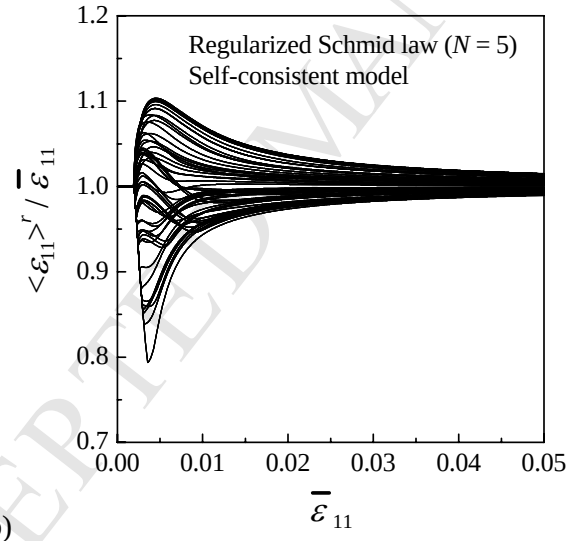

(b)

Figure A1. Influence of exponent in regularized Schmid law for isotropic non-hardening f.c.c. polycrystal. (a) Macroscopic flow stress and (b) strain heterogeneity.

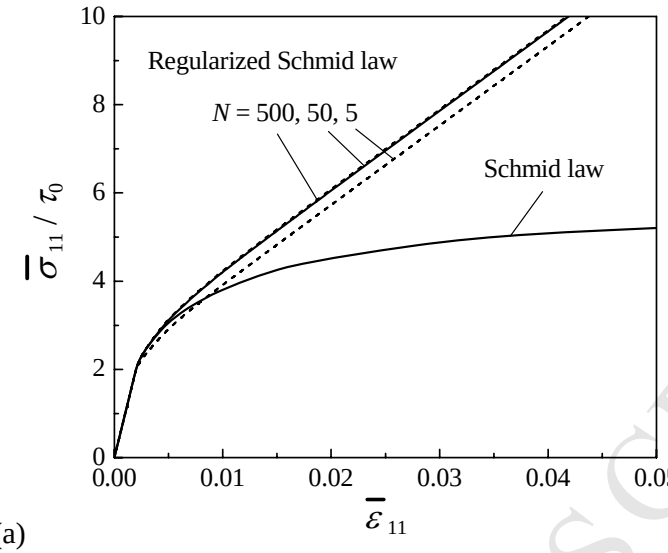

(a)

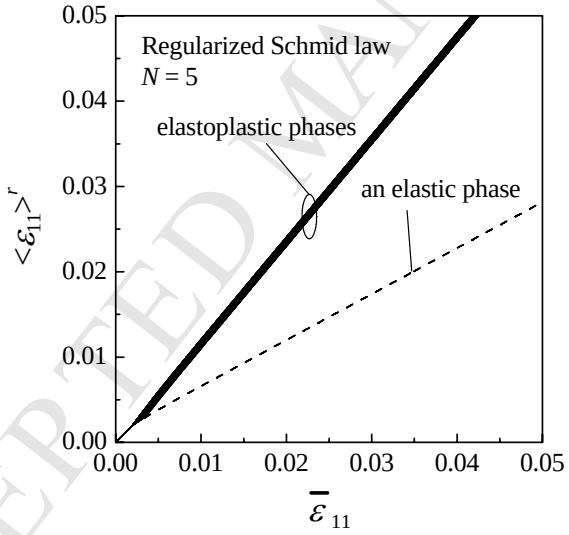

(b)

Figure A2. Influence of exponent in regularized Schmid law for isotropic non-hardening f.c.c. polycrystal reinforced by an elastic inclusion. (a) Macroscopic flow stress and (b) strain heterogeneity.